Published in final edited form as:
Ultrasound Med Biol. 2009 January ; 35(1): 65–78. doi:10.1016/j.ultrasmedbio.2008.07.001.

IN VIVO MONITORING OF FOCUSED ULTRASOUND SURGERY USING LOCAL HARMONIC MOTION

Laura Curiel, **Rajiv Chopra**, and **Kullervo Hynynen**
Imaging Research, Sunnybrook Health Sciences Centre, 2075 Bayview Ave., Toronto, ON, M4N 3M5, Canada

Abstract

The present study established the feasibility of a technique for monitoring FUS lesion formation *in vivo* using localized harmonic motion (LHM) measurements. Oscillatory motion (frequencies between 50 and 300 Hz) was generated within tissues by induction of a periodic radiation force with a focused ultrasound (FUS) transducer. The harmonic motion was estimated using cross-correlation of RF ultrasonic signals acquired at different instances during the motion by using a confocal diagnostic ultrasound transducer. The technique was evaluated *in vivo* in rabbit muscle (14 locations) in an MR imager for simultaneous ultrasound harmonic motion tracking and MR thermometry. The measured maximum amplitude of the induced harmonic motion before and after the lesion formation was significantly different for all the tested motion frequencies and decreased between 17 and 81% depending on the frequency and location. During the FUS exposure a drop in the maximum amplitude value was observed and a threshold value could be associated to the formation of a thermal lesion. A series of controlled sonications was performed by stopping the exposure when the threshold value in LHM amplitude was reached and the presence of a thermal lesion was confirmed by MR imaging. LHM measurements were also used to perform a spatial scan of the tissues across the exposure region and the thermal lesions could be detected as a reduction in the maximum motion amplitude value at the sonication region.

Keywords

Lesion; Monitoring; HIFU; FUS; Radiation force; Elastography; Tissue ablation; Ultrasound

INTRODUCTION

Focused Ultrasound Surgery (FUS) has been proposed as a noninvasive thermal therapy for diverse applications (Fry et al. 1955, Hynynen et al. 1993, ter Haar 1995). Tissue destruction is achieved through thermal coagulation resulting from a localized temperature elevation. The temperature elevation induced by ultrasound *in vivo* depends on local properties of the tissues that determine the energy absorption and the heat transfer induced by thermal conduction and blood perfusion (Billard et al. 1990, Hynynen et al. 1989). These properties can vary significantly between different tissues and within a target treatment volume. Even if the same treatment parameters are applied each time, the local properties of the tissue can lead to a

Corresponding author: Laura Curiel, Imaging Research Room C713, Sunnybrook Health Sciences Centre, 2075 Bayview Ave., Toronto, ON, M4N 3M5, Canada, laura.curiel@sri.utoronto.ca.

potential variation in clinical results (Poissonnier et al. 2007). One way to eliminate this uncertainty is to monitor and control the temperature elevation and thermal dose during the treatment. Magnetic resonance imaging (MRI) can provide temperature monitoring within tissues during a treatment, making this modality an excellent choice as a treatment control tool. Nevertheless, the cost involved in MRI-controlled treatments is high, making the search of lower cost alternatives an important goal.

One possible tissue property that has potential for use in monitoring focused ultrasound surgery is stiffness. The temperature dependence of tissue stiffness has been outlined by several authors (Chae et al. 2003, Konofagou et al. 2003, van Kleef et al. 1978). It has been shown that tissue stiffness decreases initially during heating, and starts to increase if heated above a certain temperature threshold (Heikkila and Hynynen 2006, Wu et al. 2001b). This suggests a tissue and temperature-dependent irreversible protein denaturation process. Therefore, the change of tissue stiffness could be directly related to thermal-induced coagulation and may thus be used as an indicator that adequate thermal exposure was reached.

Different attempts have been made to estimate stiffness-related parameters within tissues, such as strain measurements (Konofagou 2004, Ophir et al. 1999, Ottensmeyer 2002), tissue displacement under a localized force (Nightingale et al. 2002), response to vibration (Parker et al. 1990), and ultrasound-stimulated acoustic emission (USAE) of tissues (Fatemi and Greenleaf 1998, Fatemi and Greenleaf 1999). It has been shown that USAE can sense and map FUS lesions both in simulations (Konofagou et al. 2001) and in *in vitro* experiments (Karjalainen et al. 1999). The USAE amplitude has also been demonstrated to be sensitive to the change in temperature during heating and cooling, and before and after coagulation (Konofagou et al. 2002).

Recently, the concept of localized harmonic motion (LHM) imaging has been described (Konofagou and Hynynen 2003). The main principle behind the proposed technique is that local harmonic motion induced by an oscillatory, remotely applied, harmonically varying radiation force, can be measured in tissues. The time varying radiation force can be applied by overlapping two ultrasound beams radiating at slightly different frequencies or by radiating the tissues with amplitude modulated single-frequency ultrasound beam. The focused ultrasound exposure induces a time-varying force that induces oscillation of tissue at the frequency difference between the two beams or at the modulation frequency of the single beam (Heikkila and Hynynen 2006). The harmonic motion is estimated at different time points using cross-correlation of the RF ultrasonic signals acquired by a separate diagnostic ultrasound beam focused at the location undergoing vibration (Konofagou and Hynynen 2003). As in the USAE technique, a low frequency radiation force is used to excite tissues generating a local motion, but in LHM instead of detecting the acoustic emission induced by the excited tissues the actual movement of the tissues is tracked by a diagnostic ultrasound beam. As the estimated response is directly obtained from the tissues undergoing vibration, the information is more dependent on the tissue characteristics at the focus than on the surrounding tissue.

In Local Harmonic Motion, tissues are moved using a varying radiation force. The radiation force is periodically applied by operating the FUS transducer with a modulated excitation. The obtained motion is also periodic with a frequency predominantly comprised of the modulation fundamental. Since the movement being tracked is at the location where it was induced, the term localized harmonic motion is used. A periodic excitation was chosen since it has been observed through simulations that the obtained displacements are of higher amplitude when a steady state is reached (Heikkila and Hynynen, 2006).

This study tests the feasibility of inducing LHM within tissues *in vivo* to monitor the appearance of thermal coagulation. The overall goal is to evaluate whether LHM can be used for online thermal surgery monitoring *in vivo*.

MATERIALS AND METHODS

Experimental set-up

Two sets of experiments were performed with different focused ultrasound (FUS) transducers. For the first set of experiments a single-element focused ultrasound (FUS) transducer operating at a central frequency of 1.69 MHz was used to both induce the harmonic motion and create the lesions in tissue. The FUS transducer had a diameter of 100 mm with a central hole of 70 mm in diameter and a focal length of 80 mm. The intensity full width at half maximum (FWHM) of the transducer was 0.6 mm. For the second set of experiments a single-element FUS transducer with a 1.536 MHz central frequency was used to induce the local harmonic motion and create the lesions. This FUS transducer had also a 100-mm diameter and 80-mm focal length but the central hole had a 14-mm diameter and its intensity FWHM was 0.8 mm. Beam profiles for both transducers are shown in Figure 1.

An MRI-compatible, custom manufactured single circular element US diagnostic transducer (PZT 5, 1–3 piezocomposite, Imasonic, Besançon, France) was mounted inside the central hole of the first FUS transducer. For the second transducer with the smaller hole the diagnostic transducer was mounted in front of the central hole such that the focal volumes of the two transducers overlapped. Therefore the diagnostic transducer blocked some of the therapy beam propagation to the focus. The diagnostic transducer had a central frequency of 5 MHz, a focal length of 50 mm, a diameter of 20 mm and a bandwidth of 50% (at −3 dB in power). The focal volume of the diagnostic transducer was aligned with that of the FUS transducer to ensure the highest signal-to-noise ratio (SNR) of the signal to be tracked. To verify alignment and in order to ensure that the US diagnostic transducer was effectively observing the FUS focal point, the assembly was placed in a water tank and the ultrasound field of each transducer was measured using a needle hydrophone (0.075-mm diameter, Precision Acoustics, Dorset, UK).

The transducer assembly was mounted on an arm and introduced in a water tank facing upwards, with the target tissues at the top of the tank (Figure 2). The tank was introduced into an MR scanner (Signa SP, GE Healthcare, USA) to enable visualization of tissues before and after the sonication as well to acquire temperature maps during the sonication. In order to avoid interference between MR and ultrasound imaging signals the materials and excitation system were mounted following procedures and filtering developed by our group for a simultaneous US/MR imaging system (Curiel et al. 2007).

To induce tissue motion, the FUS transducer was excited at its central frequency by modulated bursts generated by a function generator (Agilent 3250A, Agilent, USA) and then amplified by an RF amplifier (ENI A150, ENI, USA). The key points of the induced motion are first that the motion is localized to the focus and this is where it is being tracked. Secondly, the induced motion is periodic because of the excitation. In the present study we chose an excitation where the FUS burst was modulated by an on/off square wave with a frequency between 50 and 300 Hz, 50% duty cycle. The motion generated by this kind of excitation is not purely harmonic due to the square modulation wave. However, the motion is periodic and it is predominantly comprised of the fundamental frequency of the modulation. The motion could also be induced by using a sinusoidal modulation and a purely harmonic motion would be observed. Hence the label local harmonic motion (LHM) used to describe this method.

The diagnostic US transducer was driven by a pulser/receiver (JSR300, Ultrasonics, NY, USA). Pulses were sent during the radiation force application at a pulse-repetition frequency (PRF)

of 3 kHz to track the motion of the tissue as a function of time. The data was acquired using a PCI digitizer card (ATS860, Alazartech, Canada) and stored on a hard drive. RF data was acquired for a window of 20ms (sampling frequency of 125 MHz) during the exposure corresponding to between 1 and 6 periods of the oscillatory motion.

RF signal tracking was performed using cross-correlation techniques with a 1.5-mm window. Displacement estimates were made relative to the initial position (i.e., the instant before the ultrasound exposure). The received RF signal was filtered using a high-pass filter with a cutoff frequency of 2.5 MHz to remove signal contamination from the FUS transducer. After acquisition of RF signals, a digital notch filter was also used to further filter the fundamental of the sonication frequency (1.69 MHz) as well as its harmonics. The heavy filtering implemented in this study could alter the signal, so it was performed on the whole acquired signal including the reference to reduce de-correlation. As well, the therapy and diagnostic transducers were chosen with different and distant central frequencies to reduce noise.

In vivo experiments

Seven New Zealand White rabbits (male, average weight 3.5 kg) were anesthetized using a mixture of ketamine and xylazine, and had both thighs shaved and depilated. The experiment received approval from the local Institutional Animal Care Committee. The rabbit was subsequently laid on a platform over the water tank in the lateral decubitus position and covered with a heating blanket to maintain a constant body temperature. The shaved thigh was placed over an acoustic window in front of the transducer assembly and in contact with a water bath (Figure 2). A first set of experiments was performed to analyze the feasibility of detecting the local harmonic motion in tissues before, during and after a FUS lesion formation. A total number of 14 locations were sonicated during these experiments with different exposure parameters. Multiple lesions were placed in the thigh muscle. In order to ensure no interaction between sonifications the minimum spacing between lesions was 10 mm and the time between each sonication was between 15 and 20 min. These waiting times were the ones registered during experiments but it was later observed in MR temperature maps that tissues were back to the baseline after 3 minutes for a 50-s sonication. In a regular set-up there would be no need to wait so long to repeat the exposures. A second set of experiments was performed to test the feasibility of LHM-controlled exposures. A total number of 42 locations were sonicated using this control method with different exposure parameters.

Harmonic motion before and after lesion formation

The focal point was placed within the tissues at a different depth for each target location (Table 1) with an average depth value of 18.8 ± 5.3 mm from the skin. A 50%-duty cycle burst at different repetition frequencies was delivered to the muscle in order to induce a local harmonic motion. The LHM was induced and measured at each location during 20 ms at an average acoustical power of 22.5 W. The acoustic intensity in situ was obtained from measurements using a needle hydrophone (0.075-mm diameter, Precision Acoustics, Dorset, UK) taking into account the attenuation of the muscle (4 Np/m/MHz).

The frequency dependence of the LHM signal from muscle tissue before and after sonication was investigated by obtaining LHM measurements at burst modulation frequencies between 50 and 300 Hz. Each measurement was repeated 5 times at a particular frequency with a delay of 5 s between measurements to minimize tissue heating. MR thermometry was performed during one such measurement, and a peak temperature rise of 1.4°C was measured.

Harmonic motion during lesion formation

To induce a thermal lesion at each location a FUS burst modulated at a frequency of 100Hz, 50% duty cycle and an acoustical power of 22.5 W was continuously delivered to the muscle

for 40 s. During the 40-s exposure, LHM measurements were obtained every 1.1 s. The PRF of the FUS burst signal was varied to produce temperature elevations of different magnitude and temporal evolution. Table 1 shows the sonication parameters that were used for the different experiments. MR thermometry was performed during the sonication in a plane transverse to the ultrasound beam at the focal location to obtain the tissues temperature and thermal dose and to correlate them with the harmonic motion measurements. The temperature monitoring used the temperature dependence of the proton-resonant frequency (Ishihara et al. 1995). MR thermometry was performed with a fast gradient echo sequence using the Proton Resonant Frequency shift method (FGRE, 256×128, TE/TR=17.3/34.9, FOV=16cm, Slice=3mm, Img. time=4.6 s, 1NEX). Changes in the proton-resonant frequency were estimated by measuring changes in phase and dividing by 2π times the time in which the phase developed (McDannold et al. 2000). A total of 30 images were obtained at each location before, during and after the exposure (two baselines before sonication). The temperature dependence of the proton-resonant frequency shift used for the thermometry measurements was 0.00909 ppm/°C (Chung et al. 1999). A rectal temperature probe was used to obtain the base temperature of the animal before performing MRI thermometry. MR thermometry calculations were made off-line at the end of experiments.

Controlled FUS exposures

In order to evaluate whether LHM can be used for online thermal surgery monitoring *in vivo* we performed a series of 42 controlled exposures using the same animal model. The focus was located within the tissues at different depths (average 18.1 ± 3.7 mm). For each location ten LHM amplitude measurements were performed using a FUS modulating frequency of 75 Hz. The acoustic power used for LHM measurements was chosen to have initial LHM amplitude around 20μm or more. To determine the possibility of using the LHM signal as a method to detect tissue coagulation during sonication the following post-sonication analysis of the LHM signal was performed. The mean value of the amplitude (PRE_MEAN) and standard deviation (PRE_SD) of ten repeat measurements of the LHM prior to the sonications was calculated. Then the time point when the LHM signal started to decrease during the sonication was determined as the time point when the LHM measured signal during the sonication dropped below a value DROP = PRE_MEAN−2*PRE_SD. This value was selected to ensure that the detected drop was not an artifact of the noise in the signal. The sonication was finally performed using different exposure parameters (Table 2) and LHM amplitude measurements were performed during the exposure every 1.1 s. The sonication was stopped when the LHM amplitude decreased below the threshold value of drop. For eight experiments the exposure was continued to 5s after reaching the threshold to obtain a larger lesion than the one obtained with the threshold value (Table 2). The presence of a thermal lesion was then verified using T2-weighted MR imaging (FSE, 256×256, TE/TR=69.10/2000, FOV=16cm, Slice=2.5mm, ETL=4, 1NEX).

Spatial lesion detection

The capability to produce a spatial map of the thermal lesion was evaluated by performing a linear scan of LHM measurements across the target location. This measurement was made for two of the sonications in this study. To perform the spatial scanning the LHM was induced and measured at different spatial locations. The transducer assembly was scanned in order to place the FUS transducer focus at a different location each time. The scan direction was transverse to the lesion and over a distance of 30 mm at 1-mm steps. At each location three burst frequencies (50, 100 and 200 Hz) were used to induce and measure the LHM with three repetitions per measurement.

RESULTS

Harmonic motion before and after lesion formation

All of the 40-s sonications delivered to the muscle produced thermal coagulation as verified by MRI T2-weighted images and post-mortem macroscopic examination. T2-weighted images of thermally induced coagulation in tissue were observed as dark regions surrounded by a bright rim as has been shown previously to correlate well with postmortem examination results (Chung et al. 1999, Hynynen et al. 1993).

Figure 3 shows the average and standard deviation of the harmonic motion amplitude for each location before and after the sonication for three different burst frequencies. A statistically significant reduction in the amplitude of harmonic motion was observed after each sonication at all locations. The amplitude of LHM reduced as a function of modulation frequency for both before and after tissue coagulation experiments. This dependence of amplitude as a function of modulation frequency is related to the tissues natural response. This dependence has already been observed when inducing local harmonic motion in phantoms and in vitro tissues (Konofagou et al., 2003) and is consistent with simulations results (Heikkila and Hynynen, 2006). Figure 4 shows an example of tissue displacement as function of time for location No. 6 before and after lesion formation.

The LHM amplitude of each experiment was normalized to its maximum value and average of normalized values for all the experiments was calculated. Figure 5 shows the average of the normalized LHM amplitude as a function of frequency for all of the experiments. The vertical bars represent the standard deviation of the normalized values between different experiments. A decrease in LHM amplitude was observed as a function of the burst frequency.

Harmonic motion during the lesion formation

The LHM amplitude and the temperature maps were obtained during the sonications. Figure 6 shows an MRI temperature map across the focus at the end of the sonication (a) and the corresponding T2-weighted MR image of location No. 13 after the sonication (b). Figure 6 (c) shows the temperature rise at the focus and the normalized LHM amplitude as a function of time for this location. The temperature rise was averaged for a region of interest (ROI = 0.63 × 0.63 mm, equal to one voxel) close to the size of the FWHM (0.6 × 0.6 mm) of the ultrasound beam at the focus. The temperature rise is represented as a continuous line with round markers and corresponds to the left axis. The normalized LHM amplitude is represented as a dashed line with cross markers and corresponds to the right axis of the plot. In this experiment a peak temperature rise of 29 °C was observed at 43.8 s. The harmonic motion amplitude had an initial value of 34.3 ± 3.6μm and it started to decrease at 9.3 s to reach a final value of 16.8 ± 1.0μm ($p=0.01$) at the end of the sonication. For these experiments, LHM measurements were stopped at the end of the HIFU application. However, during a practical application such as a treatment control system, measurements could be continued after the sonication is finished as long as the applied average energy is low enough to avoid increasing the thermal dose. As well, treatment results could be assessed by imaging the tissues using LHM measurements when mechanically moving the transducer assembly.

To test if the initial LHM amplitude drop during the sonication can be used as an indicator of tissue coagulation, the temperature, thermal dose and normalized LHM amplitude were calculated from the MRI thermometry data at the moment when the harmonic motion amplitude drop was detected for all sonications (time point when the LHM signal dropped below PRE_MEAN−2*PRE_SD values). Figure 7 shows the temperature (a) and thermal dose (b) obtained for all the locations at the instant when the harmonic motion amplitude decrease was first detected. The drop in the LHM amplitude values seemed to occur over a reasonably

consistent range of temperatures and thermal dose values. The average temperature value where the drop was obtained was 53 ± 1.3 °C with a decrease in temperature as a function of time. The average thermal dose at threshold was 29 ± 10 equivalent minutes at 43°C (Sapareto and Dewey 1984) and spanned between 18 and 51 equivalent minutes at 43°C. The drop in the LHM amplitude reflects an increase in stiffness (Konofagou et al., 2003). This increased stiffness is obtained at different durations of sonications in different locations. However, the temperature and thermal dose achieved when the drop happened were constant.

Controlled FUS exposures

Over the 42 controlled exposures performed, 34 lesions appeared when the sonication was stopped at the threshold. The appearance of a lesion was confirmed by MR images and macroscopic examination. For six locations the LHM amplitude measured 1.1s after starting the exposure was lower that the threshold and the system stopped without obtaining any lesion. For two locations (27 and 28) we intentionally moved to locations where a lesion was already present and a new controlled exposure was performed. In these two cases the LHM amplitude during the exposure never dropped below the threshold and the exposure continued to the maximum allowed time (50 s). Table 2 also shows the results obtained for the 42 controlled exposures with the time needed to reach the threshold.

Figure 8 shows the acoustic intensity at the focus versus the exposure time needed to reach the LHM threshold for the controlled exposures. The dispersion was high showing differences in the necessary exposure time to obtain tissue coagulation depending on the location. Even if the trend was as expected, and an increased acoustic intensity required less exposure time to coagulate tissues, there was no statistical correlation. This can be explained by tissue inhomogeneities that cause differences in the needed exposure to obtain coagulation and shows the importance of direct measurements to monitor FUS ablation.

Figure 9 shows a sagittal MR image corresponding to the controlled exposures Nos. 22 to 27 before any sonication was made, after five exposures at different locations were made (Nos. 22 to 26) and after one more exposure was performed (No. 27) at the same location as the previous one (No. 26). For exposures 23 and 24 no lesion was observed as the system stopped 1.1s after starting the exposure. Exposure 22 and 25 were successfully controlled. Lesions 25 and 26 are an example of sonications that were performed by continuing the exposure for 5 s after the drop was reached. Exposures 23 and 24 are two of the 6 cases where the control failed and the first measurement made at 1.1 s showed a value in LHM amplitude significantly below the pre-sonication without any coagulation observed. The intended locations for these exposures are shown with arrows where increased signal intensity is observed in the MR image, in the ultrasound signal a high amplitude echo was observed at the focus of the therapy transducer. Lesion 27 was intentionally located at the same position and the system did not register a value in LHM amplitude below the threshold, so the exposure continued to the maximum allowed time of 50s. Lesion 27 appeared in the image and in macroscopic examination as a large coagulated region.

Spatial lesion detection as a LHM amplitude reduction

Figure 10 shows the results of a linear scan over a target region with two sonications (locations Nos. 13 and 14). The corresponding sagittal (b) and coronal (c) T2-weighted MR images of the lesions are also shown. The sonications were performed at the same focal depth and 10-mm apart along the scan direction (superior/inferior). At the boundary between non-coagulated tissue and lesion higher values of LHM amplitude were registered. LHM values come back to baseline values (before lesion formation) when moving away from the coagulated region. The drop in the LHM amplitude was correlated with the presence of the lesions. The same result was obtained at the other scanned location.

DISCUSSION

This study demonstrates for the first time the feasibility of acquiring LHM measurements *in vivo*. The consistent reduction in LHM measurements after each sonication demonstrates that radiation force-induced tissue motion is a sensitive measure of the thermal coagulation of the tissue and thus provides a tool to control the ultrasound exposures. In addition, the localized measurement of tissue properties achieved with this technique enabled spatial mapping of the location of thermally coagulated tissue. Similar techniques have been suggested and some devices have been designed with this purpose (Zaitsev et al. 2004) but *in vivo* applications have not been performed.

A decrease in the local harmonic motion amplitude as a function of increasing frequency was systematically observed at all locations regardless of the local characteristics or presence of tissue coagulation. This tendency could be observed even when the amplitude dropped to low values and the measurements were affected by noise. This dependency is related to the natural response of tissues to radiation force; tissues will move when the force is applied and go back to the steady position when it is released. When this is repeated periodically a harmonic motion is obtained and the higher the frequency the shorter the time the force is applied before release. The result is that tissues do not move as far as they would for lower frequencies thus resulting in lower amplitude at higher frequencies. This observation agrees with our earlier computer simulation studies (Heikkila and Hynynen 2006) and suggests the implementation of lower frequencies for increased motion generation and thus higher signal to noise ratio (SNR) in the measurement. However, even if lower frequencies give higher SNR, it makes necessary to increase the acquisition time to obtain the same number of cycles. Besides, for lower modulation frequencies, the tissue response approaches to a steady, non harmonic response. Therefore, a compromise should be found between frequency and SNR when implementing LHM applications.

The amplitude of the motion was different for each experiment showing a dependency on the location. This variation could be explained in part by the differences in the depth associated with attenuation. However, for some locations at the same depth the obtained value was different showing that the local elastic characteristics of the tissue changed the amplitude of the induced harmonic motion.

Two different transducers were used for the experiments with different beam profiles (Figure 1). For both transducers the observed maximum amplitudes were similar at the focus for the same acoustic power. The main difference was observed in the depth direction as we could induce movement in a longer area for the transducer with a longer axial beam-width. The reason for this difference was a distinct focal volume for the transducers. However, the described method analyzes the localized movement at the focus, thus being less dependent on the beam shape, especially when analyzing relative results between before and after coagulation.

For this study, it was found that the beginning of the LHM amplitude drop, as detected with our measurement system, happened at thermal dose values that were the same or higher than the threshold values reported earlier in rabbit muscle using ultrasound heating and MRI thermometry (McDannold et al. 2000). To be more specific the thermal doses at the detected LHM signal drop were between 18 and 51 equivalent minutes at 43°C. In (McDannold et al. 2000) study, the thermal dose values at the threshold where tissue damage always occurred was greater than 31.2 equivalent minutes at 43°C, and no tissue damage was observed for doses under 4.3 equivalent minutes at 43°C. At the LHM threshold value determined in our present study, the observed temperature values were above 51 °C with the temperatures reducing as a function of time at the rate of 0.113 °C/s. The reduction in the registered temperature when the stiffness changes appear later in exposure time can be explained by a thermal dose effect

(Sapareto and Dewey 1984) that indicates that the tissue damage threshold temperature is reduced when the exposure time is increased. Based on this observation the LHM signal may provide a method for detecting tissue coagulation and may thus be useful for exposure control.

It was possible to perform controlled exposures using local harmonic motion amplitude measurements. However, in six occasions out of 42 the first LHM amplitude measured after starting the exposure was below the threshold without any coagulation being obtained. All these locations were correlated with a high signal intensity region in the MR images and a high echo in the RF signal. After macroscopic, post mortem examination conjunctive tissue was found at these locations. A possible explanation for the observed behavior of the system is that the sonicated tissues at the focus had a high content of collagen that hardened as soon as the exposure started and the measured LHM amplitude immediately dropped.

For the locations where a lesion was already present and a second controlled exposure was performed the system never registered a value of LHM amplitude below the threshold. The LHM amplitude from coagulated tissue was significantly lower that normal tissue but additional exposure to the ultrasound did not cause extra hardening.

The observed trend in Figure 8 for the time needed to reach the LHM threshold as a function of the acoustic intensity was as expected but with a high dispersion. This dispersion suggests that the local characteristics of the tissue not only influence the value of the LHM amplitude measured before coagulation, but also their response to heat and the values of LHM obtained while heating. According to Figure 8 there is therefore a poor correlation between acoustic intensity and exposure time needed for necrosis. This confirms that establishing an exposure time based on the applied acoustic intensity is not an appropriate strategy for FUS therapy. Therefore other methods of control have to be proposed as temperature rise (Chopra et al. 2008), thermal dose (McDannold et al. 2000), or the here proposed method of harmonic motion amplitude. The measurements of LHM amplitude are directly related to the local characteristics of the tissue, therefore giving an in situ measurement of tissue coagulation that is more reliable for the exposure control than standard acoustic intensity calculations.

The proposed control system has a limitation when the focus is located in areas where the local characteristics of the tissue can make the elastic characteristics of the tissues under heating are either unchanging or change abruptly. For these cases the exposure would either continue without stopping (as when coagulation was already present) or stop immediately without any lesion formation. This could be the case either when the focus is located in conjunctive tissue (fat or collagen) or in a region already coagulated. It remains to test the exposure control when harder tissues such as tumors are sonicated to validate that the stiffness changes can successfully be observed and measured.

The spatial scan of the LHM amplitude after sonication could locate the position of the thermally coagulated tissue. The drop in the LHM amplitude correlated with the presence of the lesions that were detected by the T2-weighted MR images. This indicated that the method could be used to map the volume of the coagulated tissue and could potentially be useful also for tumor detection. The distal end of the lesion can be detected by analyzing the displacements in the depth direction. It could be nevertheless necessary to displace the focal point in depth to improve the detection. Moreover, as for other relative stiffness methods, a limitation for lesion detection is having a lesion as stiff as the surrounding tissues.

Imaging methods based on tissue elastic parameters are a natural choice for monitoring thermal therapy and visualization of thermal damage because of the large changes in elastic parameters in the coagulated tissues. Different approaches have been proposed to visualize elastic properties of thermal lesions. Acoustic radiation force impulse imaging involves the mechanical excitation of tissue using a localized, impulsive radiation force and then track tissue

displacements by using ultrasonic correlation-based methods to evaluate stiffness (Nightingale et al. 2002, Nightingale et al. 2003). This imaging has been used to visualize thermally- and chemically-induced lesions *ex vivo* and to monitor radiofrequency (RF) ablation of ovine cardiac tissue *in vivo* allowing determination of lesion location, shape, and relative size through time (Fahey et al. 2004, Fahey et al. 2005). The advantage of the technique proposed in the present paper is that the lesion formation could be followed in shorter time steps and the same applicator was used to interrogate and to treat tissues.

Vibro-acoustography has also been used to image mass lesions in *ex vivo* soft tissue showing images with an enhanced boundary and distinctive textures relative to their background (Alizad et al. 2004). Vibro-acoustography has shown a strong temperature dependence of the signal amplitude during *ex vivo* tissue heating (Karjalainen et al. 1999). However, this technique requires the use of a hydrophone to detect the signal, making an *in vivo* or clinical application challenging. For vibro-acoustography as well as for LHM, the response from tissues under excitation can be affected by surrounding tissues as the induced movement is affected by the neighboring structures. The changed movement will modify the emission detected in vibro-acoustography and the tracked movement detected in LHM. However, in vibro-acoustography the tissue motion is induced by continuous wave sonication and it is detected by the acoustic signal measured by an external hydrophone. Thus, the method is sensitive to ambient noise and to standing waves, as well as reflected and scattered ultrasound signals that can influence the detected acoustic signal amplitude. On the other hand, LHM would be sensible to any movements that displace tissues out of the axis where echoes are tracked.

Another proposed method is ultrasound-based elastography or sonoelastography, where strain images are obtained by continuously compressing tissues while ultrasound RF signal is acquired and displacements are then obtained by cross-correlation techniques. Ultrasound-induced thermal lesions have been visualized *in vitro* using elastography and a correlation to gross pathology analysis was found (Kallel et al. 1999). Sonoelastography has also been used *in vivo* for prostate cancer ultrasound-therapy evaluation; the thermally-treated regions could be depicted in the strain images and correlated to MR images (Curiel et al. 2005, Souchon et al. 2003). Sonoelastography of RF ablation thermal lesions by using the RF probe as the compressor/displacement device has also been successfully done (Varghese et al. 2002). Magnetic Resonance Elastography (MRE) has also been used to perform tissue elasticity images. MRE can be performed by using external compression or by using ultrasound transducers to induce a local motion as the one proposed in the present study. MRE has been used to visualize focused ultrasound ablated tissue in *ex vivo* bovine muscle (Wu et al. 2001a) and it has been proposed as a monitoring tool of MRI-guided focused ultrasound thermal therapy (Le et al. 2006, Lizzi et al. 2003, Maleke et al. 2006), but no *in vivo* application has been performed.

The noise in the acquired signal was found to be an important issue during this study. Filtering the FUS frequency and its harmonics allowed reducing the noise and eliminating de-correlation that could result in incorrect displacement calculations. Having the therapy and diagnostic transducers with very different central frequency was useful to reduce noise. Another possibility would have been to collect data only during OFF time; however, the maximum displacement occurs during the ON and it would be therefore missed, reducing the SNR of the technique.

Other sources of noise for the technique can come from changes in the RF signal causing de-correlation. These include out-of-plane movements, expansion/compression of tissues or changes in the nature of tissues that alter the echo shape. However, by acquiring at high PRF, the de-correlation can be minimized as very small movements are tracked every time. As well, the measuring times are relatively short (around 30 ms), making the technique less sensitive

to large and usually slower movements. However, movements from heart beats, breathing, blood flow and digestive tract could become more significant if considering the application of this technique in fast-moving organs like heart, liver and some vessels.

Finally, this study was only performed on normal muscle tissue. Future work needs to be conducted to verify that the same changes can be observed and detected during an FUS exposure on other tissues as well as in tumors. Additionally, the LHM technique may also be useful for diagnostic purposes since many tumors are stiffer than the surrounding tissues (Krouskop et al. 1998, Samani et al. 2007).

Acknowledgements

This work was supported partially by CRC and NIH R21/R33 CA102884-01 and a program project grant from Terry Fox foundation.

References

Alizad A, Wold LE, Greenleaf JF, Fatemi M. Imaging mass lesions by vibro-acoustography: modeling and experiments. IEEE Trans Med Imaging 2004 Sep;23(9):1087–93. [PubMed: 15377117]

Billard BE, Hynynen K, Roemer RB. Effects of physical parameters on high temperature ultrasound hyperthermia. Ultrasound Med Biol 1990;16(4):409–20. [PubMed: 2396329]

Chae Y, Aguilar G, Lavernia EJ, Wong BJ. Characterization of temperature dependent mechanical behavior of cartilage. Lasers Surg Med 2003;32(4):271–8. [PubMed: 12696094]

Chopra R, Baker N, Choy V, Boyes A, Tang K, Bradwell D, Bronskill MJ. MRI-compatible transurethral ultrasound system for the treatment of localized prostate cancer using rotational control. Med Phys 2008;35(4):1346–57. [PubMed: 18491529]

Chung AH, Jolesz FA, Hynynen K. Thermal dosimetry of a focused ultrasound beam in vivo by magnetic resonance imaging. Med Phys 1999 Sep;26(9):2017–26. [PubMed: 10505893]

Curiel L, Chopra R, Hynynen K. Progress in Multimodality Imaging: Truly Simultaneous Ultrasound and Magnetic Resonance Imaging. IEEE Trans Med Imaging. in press

Curiel L, Souchon R, Rouviere O, Gelet A, Chapelon JY. Elastography for the follow-up of high-intensity focused ultrasound prostate cancer treatment: initial comparison with MRI. Ultrasound Med Biol 2005 Nov;31(11):1461–8. [PubMed: 16286025]

Fahey BJ, Nightingale KR, McAleavey SA, Palmeri ML, Wolf PD, Trahey GE. Acoustic radiation force impulse imaging of myocardial radiofrequency ablation: initial in vivo results. IEEE Trans Ultrason Ferroelectr Freq Control 2005 Apr;52(4):631–41. [PubMed: 16060512]

Fahey BJ, Nightingale KR, Stutz DL, Trahey GE. Acoustic radiation force impulse imaging of thermally- and chemically-induced lesions in soft tissues: preliminary ex vivo results. Ultrasound Med Biol 2004 Mar;30(3):321–8. [PubMed: 15063514]

Fatemi M, Greenleaf JF. Application of radiation force in noncontact measurement of the elastic parameters. Ultrason Imaging 1999 Apr;21(2):147–54. [PubMed: 10485567]

Fatemi M, Greenleaf JF. Ultrasound-stimulated vibro-acoustic spectrography. Science 1998 Apr 3;280 (5360):82–5. [PubMed: 9525861]

Fry WJ, Barnard JW, Fry FJ, Brennan JF. Ultrasonically produced localized selective lesions in the central nervous system. Am J Phys Med 1955 Jun;34(3):413–23. [PubMed: 14376518]

Heikkila J, Hynynen K. Investigation of optimal method for inducing harmonic motion in tissue using a linear ultrasound phased array--a simulation study. Ultrason Imaging 2006;28(2):97–113. [PubMed: 17094690]

Hynynen K, Darkazanli A, Unger E, Schenck JF. MRI-guided noninvasive ultrasound surgery. Med Phys 1993 Jan–Feb;20(1):107–15. [PubMed: 8455489]

Hynynen K, DeYoung D, Kundrat M, Moros E. The effect of blood perfusion rate on the temperature distributions induced by multiple, scanned and focused ultrasonic beams in dogs' kidneys in vivo. Int J Hyperthermia 1989 Jul–Aug;5(4):485–97. [PubMed: 2746052]

Ishihara Y, Calderon A, Watanabe H, Okamoto K, Suzuki Y, Kuroda K, Suzuki Y. A precise and fast temperature mapping using water proton chemical shift. Magn Reson Med 1995;34(6):814–823. [PubMed: 8598808]

Kallel F, Stafford RJ, Price RE, Righetti R, Ophir J, Hazle JD. The feasibility of elastographic visualization of HIFU-induced thermal lesions in soft tissues. Image-guided high-intensity focused ultrasound. Ultrasound Med Biol 1999 May;25(4):641–7. [PubMed: 10386741]

Karjalainen, T.; Thierman, JS.; Hynynen, K. Ultrasound acoustic stimulated emission for controlling thermal surgery. Ultrasonics Symposium Proceedings; IEEE; 1999 Oct. 17. Oct. 17. p. 1397-1400.

Konofagou E, Thierman J, Hynynen K. The use of ultrasound-stimulated acoustic emission in the monitoring of modulus changes with temperature. Ultrasonics 2003 Jul;41(5):337–45. [PubMed: 12788215]

Konofagou E, Thierman J, Hynynen K. A focused ultrasound method for simultaneous diagnostic and therapeutic applications--a simulation study. Phys Med Biol 2001 Nov;46(11):2967–84. [PubMed: 11720358]

Konofagou EE. Quo vadis elasticity imaging? Ultrasonics 2004 Apr;42(1–9):331–6. [PubMed: 15047307]

Konofagou EE, Hynynen K. Localized harmonic motion imaging: theory, simulations and experiments. Ultrasound Med Biol 2003 Oct;29(10):1405–13. [PubMed: 14597337]

Konofagou EE, Thierman J, Karjalainen T, Hynynen K. The temperature dependence of ultrasound-stimulated acoustic emission. Ultrasound Med Biol 2002 Mar;28(3):331–8. [PubMed: 11978413]

Krouskop TA, Wheeler TM, Kallel F, Garra BS, Hall T. Elastic moduli of breast and prostate tissues under compression. Ultrason Imaging 1998 1998;20(4):260–74.

Le Y, Glaser K, Rouviere O, Ehman R, Felmlee JP. Feasibility of simultaneous temperature and tissue stiffness detection by MRE. Magn Reson Med 2006 Mar;55(3):700–5. [PubMed: 16463357]

Lizzi FL, Muratore R, Deng CX, Ketterling JA, Alam SK, Mikaelian S, Kalisz A. Radiation-force technique to monitor lesions during ultrasonic therapy. Ultrasound Med Biol 2003 Nov;29(11):1593–605. [PubMed: 14654155]

Maleke C, Pernot M, Konofagou EE. Single-element focused ultrasound transducer method for harmonic motion imaging. Ultras Imaging 2006;28:144–158.

McDannold NJ, King RL, Jolesz FA, Hynynen KH. Usefulness of MR imaging-derived thermometry and dosimetry in determining the threshold for tissue damage induced by thermal surgery in rabbits. Radiology 2000 Aug;216(2):517–23. [PubMed: 10924580]

Nightingale K, McAleavey S, Trahey G. Shear-wave generation using acoustic radiation force: in vivo and ex vivo results. Ultrasound Med Biol 2003 Dec;29(12):1715–23. [PubMed: 14698339]

Nightingale K, Soo MS, Nightingale R, Trahey G. Acoustic radiation force impulse imaging: in vivo demonstration of clinical feasibility. Ultrasound Med Biol 2002 Feb;28(2):227–35. [PubMed: 11937286]

Ophir J, Alam SK, Garra B, Kallel F, Konofagou E, Krouskop T, Varghese T. Elastography: ultrasonic estimation and imaging of the elastic properties of tissues. Proc Inst Mech Eng [H] 1999;213(3):203–33.

Ottensmeyer MP. In vivo measurement of solid organ visco-elastic properties. Stud Health Technol Inform 2002;85:328–33. [PubMed: 15458110]

Parker KJ, Huang SR, Musulin RA, Lerner RM. Tissue response to mechanical vibrations for “sonoelasticity imaging”. Ultrasound Med Biol 1990;16(3):241–6. [PubMed: 2194336]

Poissonnier L, Chapelon JY, Rouviere O, Curiel L, Bouvier R, Martin X, Dubernard JM, Gelet A. Control of prostate cancer by transrectal HIFU in 227 patients. Eur Urol 2007 Feb;51(2):381–7. [PubMed: 16857310]

Samani A, Zubovits J, Plewes D. Elastic moduli of normal and pathological human breast tissues: an inversion-technique-based investigation of 169 samples. Phys Med Biol 2007 2007;52(6):1565–76.

Sapareto SA, Dewey WC. Thermal dose determination in cancer therapy. Int J Radiat Oncol Biol Phys 1984 Jun;10(6):787–800. [PubMed: 6547421]

Souchon R, Rouviere O, Gelet A, Detti V, Srinivasan S, Ophir J, Chapelon JY. Visualisation of HIFU lesions using elastography of the human prostate in vivo: preliminary results. Ultrasound Med Biol 2003 Jul;29(7):1007–15. [PubMed: 12878247]

ter Haar G. Ultrasound focal beam surgery. Ultrasound Med Biol 1995;21(9):1089–100. [PubMed: 8849823]

van Kleef FS, Boskamp JV, van den Tempel M. Determination of the number of cross-links in a protein gel from its mechanical and swelling properties. Biopolymers 1978 Jan;17(1):225–35. [PubMed: 623882]

Varghese T, Zagzebski JA, Lee FT Jr. Elastographic imaging of thermal lesions in the liver in vivo following radiofrequency ablation: preliminary results. Ultrasound Med Biol 2002 Nov–Dec;28(11–12):1467–73. [PubMed: 12498942]

Wu T, Felmlee JP, Greenleaf JF, Riederer SJ, Ehman RL. Assessment of thermal tissue ablation with MR elastography. Magn Reson Med 2001a Jan;45(1):80–7. [PubMed: 11146489]

Wu T, Felmlee JP, Greenleaf JF, Riederer SJ, Ehman RL. Assessment of thermal tissue ablation with MR elastography. Magn Reson Med 2001b Jan;45(1):80–7. [PubMed: 11146489]

Zaitsev A, Raymond S, Thierman J, Juste J, Hynynen K. Focused ultrasound thermal surgery, imaging, and elastometry using the same phased array: feasibility study. Ultrasonics Symposium Proceedings, 2004 IEEE Aug 23–27;2004 3:2231–2234.

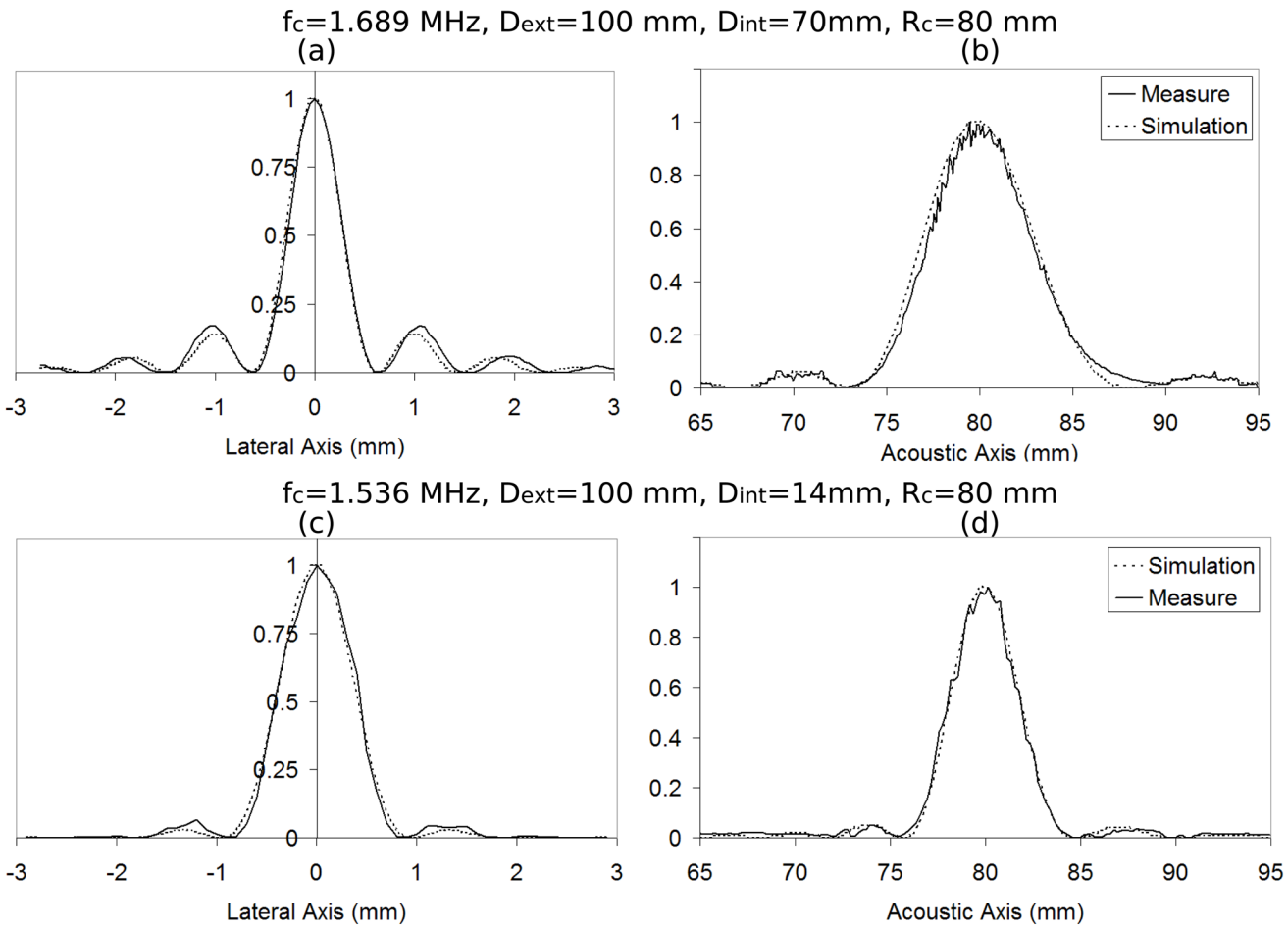

Figure 1.

Beam profiles: (a) lateral and (b) acoustical axis for transducer with 1.689 MHz central frequency (f_c), external diameter (D_{ext}) of 100 mm, internal diameter (D_{int}) of 70 mm and geometrical focus (R_c) of 80 mm; (c) lateral and (d) acoustical axis for transducer with 1.536 MHz central frequency (f_c), external diameter (D_{ext}) of 100 mm, internal diameter (D_{int}) of 14 mm and geometrical focus (R_c) of 80 mm.

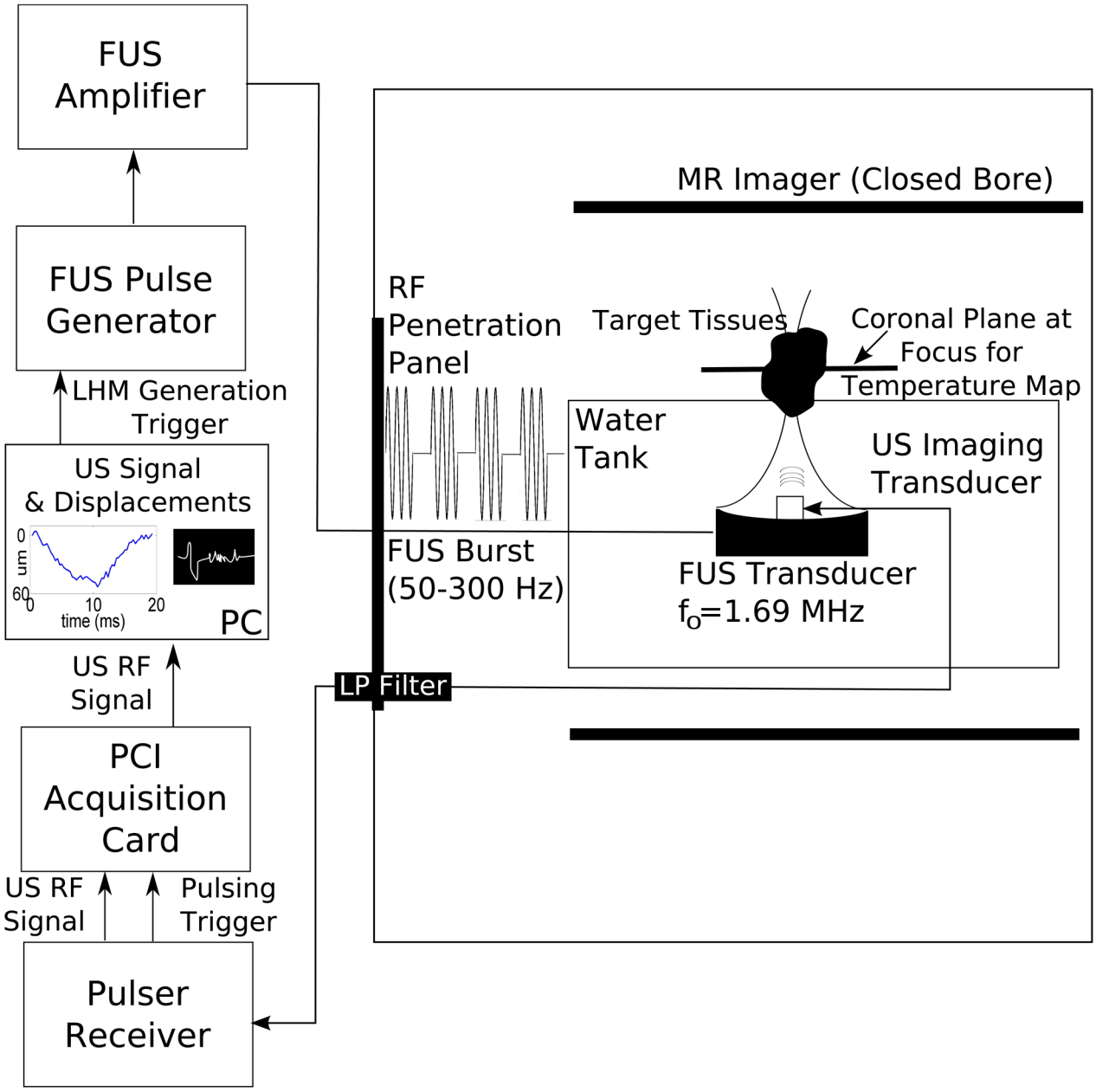

Figure 2.

Experimental set-up used for the LHM measurements. FUS and diagnostic transducer assembly were placed in a water tank facing up, with the target tissues on top of the tank. The tank was introduced into the MR Imager to allow visualization of tissues and temperature maps during the sonication. Materials inside the tank were MR-compatible; the excitation system was outside the MR room and the signals were introduced into the MR room through a penetration panel using filtering when necessary.

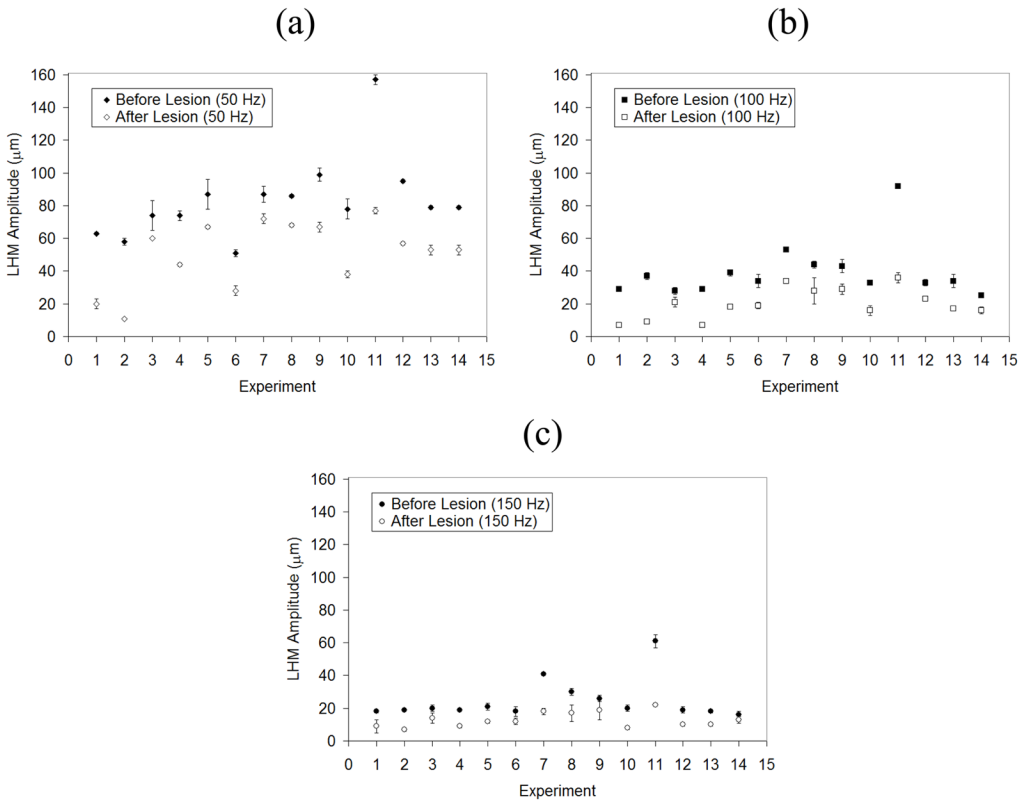

Figure 3.
Harmonic motion amplitude for each of the fourteen locations studied before and after sonication at three different modulation frequencies (50, 100 and 150 Hz). The values shown are the average of 5 measures at each location; error bars show the standard deviation.

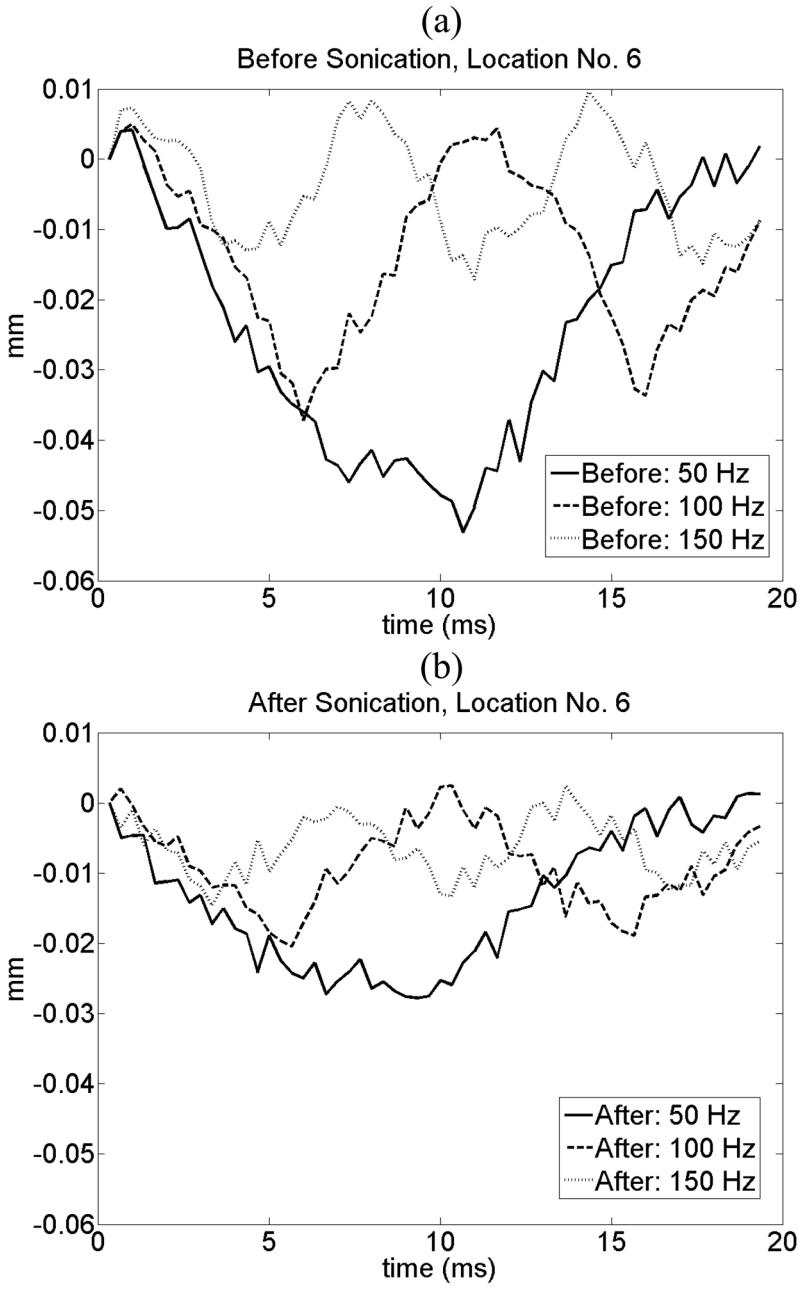

Figure 4.
Example of tissue displacement (in mm) at location No. 6 as a function of time (a) before and (b) after lesion formation. The results for a 50, 100 and 150 Hz burst are presented. The amplitude decreases after lesion formation for all the frequencies.

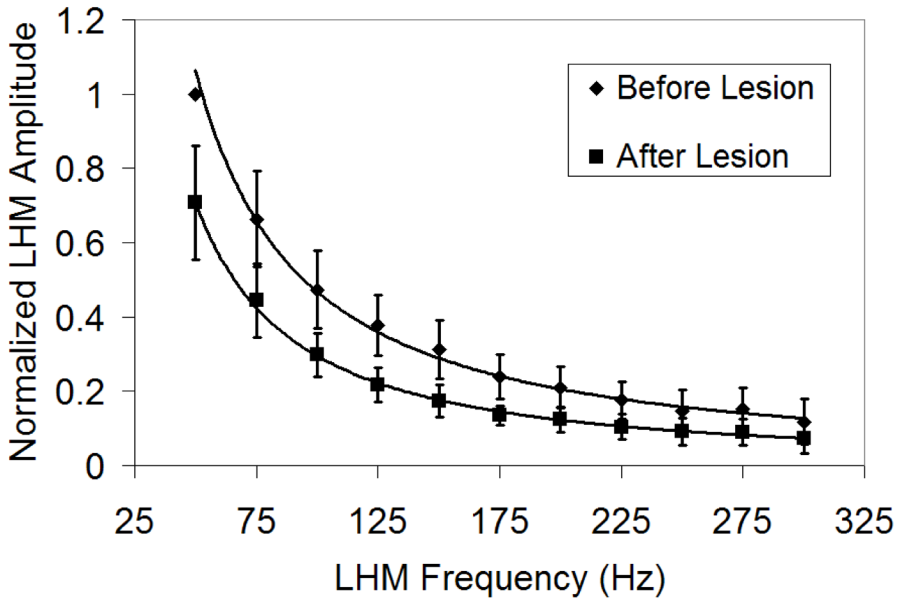

Figure 5.

Average of normalized LHM amplitude as a function of frequency for all the experiments. The motion amplitude was normalized by the maximum value obtained at each location (50 Hz burst before lesion formation). The difference between before and after lesion formation was significant for all the frequency bursts (50 Hz, $p<0.0001$; 75 Hz, $p<0.0001$; 100 Hz, $p<0.0001$; 125 Hz, $p<0.0001$; 150 Hz, $p<0.0001$; 175 Hz, $p<0.0001$; 200 Hz, $p=0.0001$; 225 Hz, $p=0.0005$; 250 Hz, $p=0.008$; 275 Hz, $p=0.004$; 300 Hz, $p=0.04$).

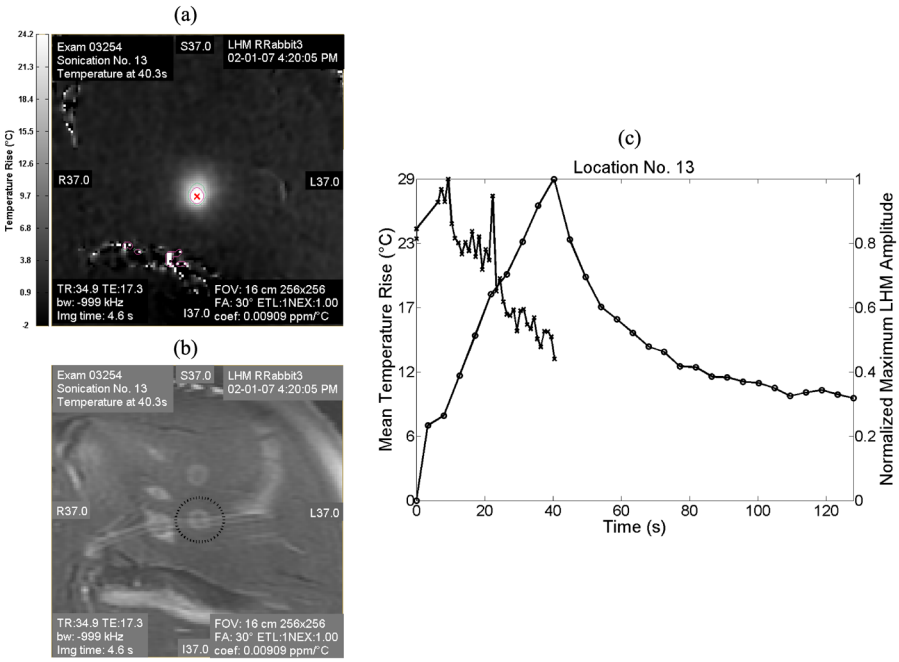

Figure 6.

Temperature and LHM amplitude during the sonication for the location No. 13. (a) MRI temperature map (coronal) at the end of the sonication (43.8 s) and (b) corresponding T2-MR image after the sonication. (c) Plot of the temperature rise at the focus (left axis, round markers with continuous line) and of the normalized LHM amplitude (right axis, cross markers with dashed line) as a function of time for the same location.

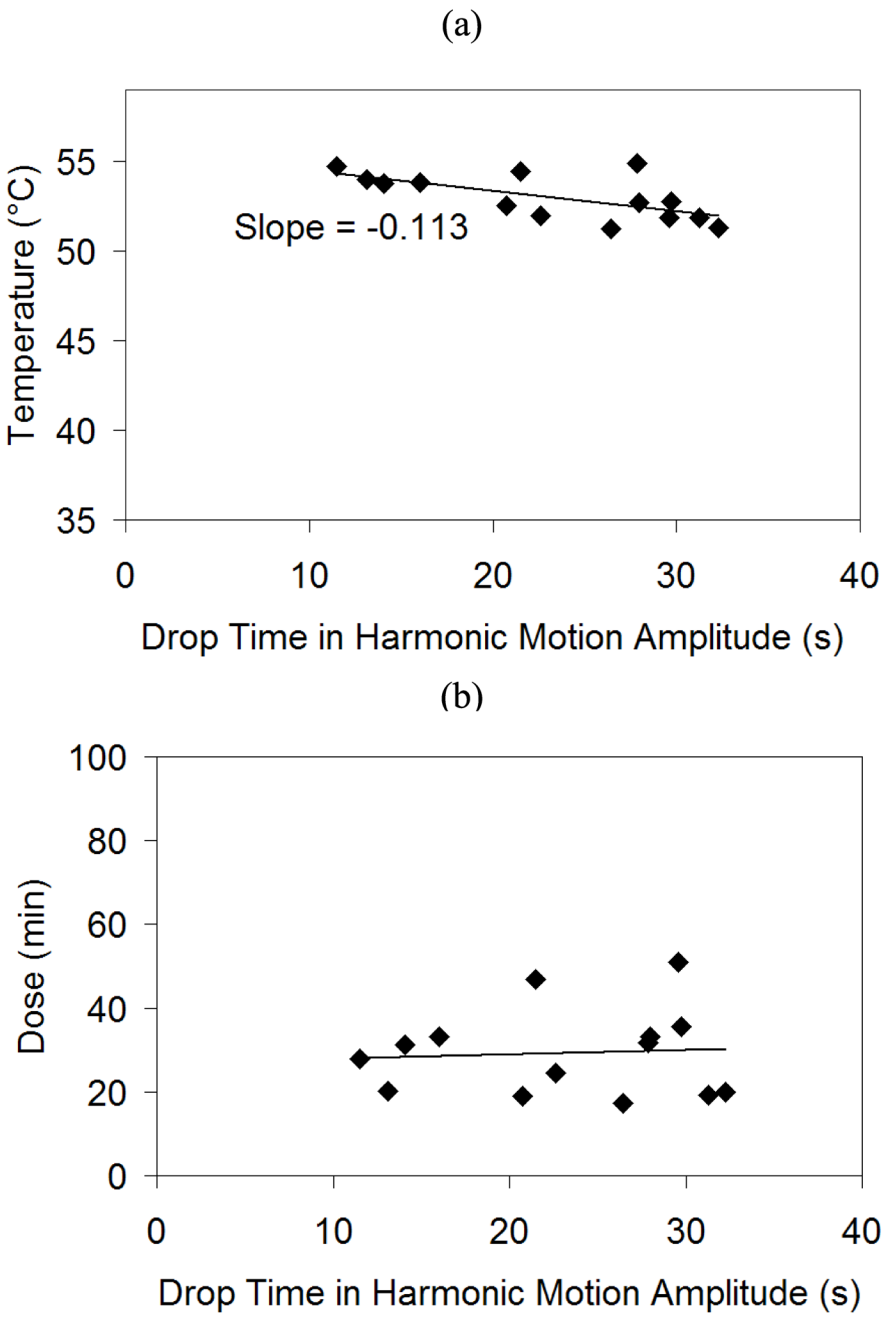

Figure 7.
Temperature (a) and dose (b) for all the locations at the instant when the harmonic motion dropped below the threshold.

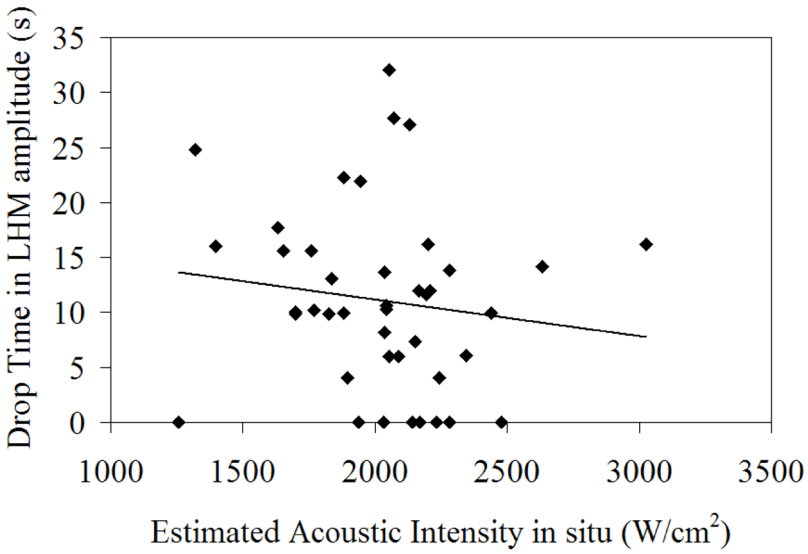

Figure 8.
Time to reach the threshold during the controlled exposures experiments as a function of the acoustic intensity in situ of the exposure.

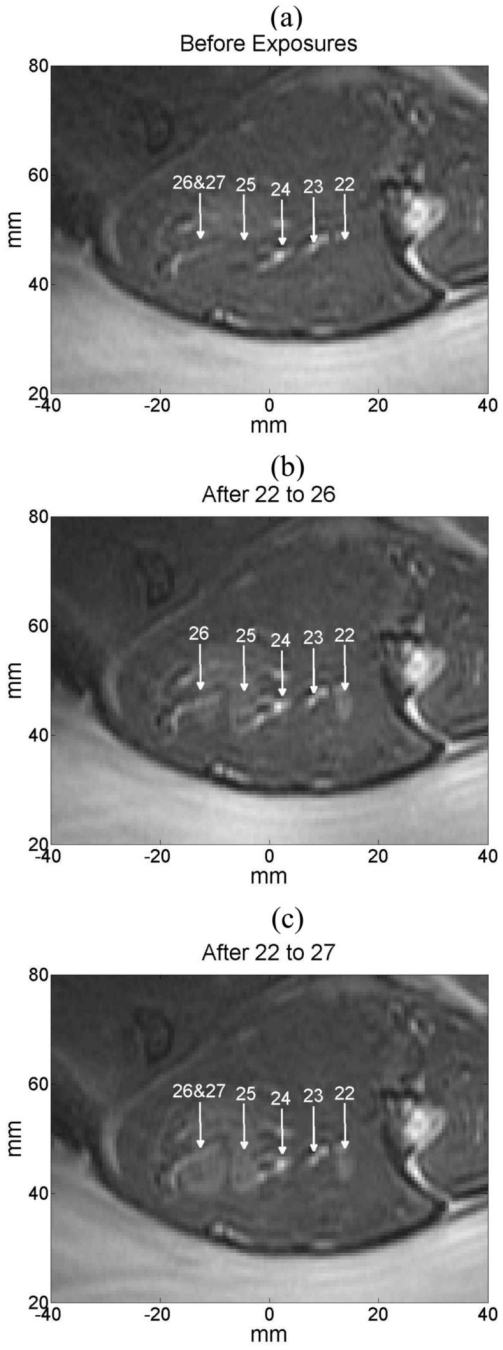

Figure 9.
MR sagittal image where controlled exposures No. 22 to 27 (a) before any sonication was performed, (b) after exposures 22 to 26 were made, and (c) when exposure 27 was made (at the same location as exposure 26.

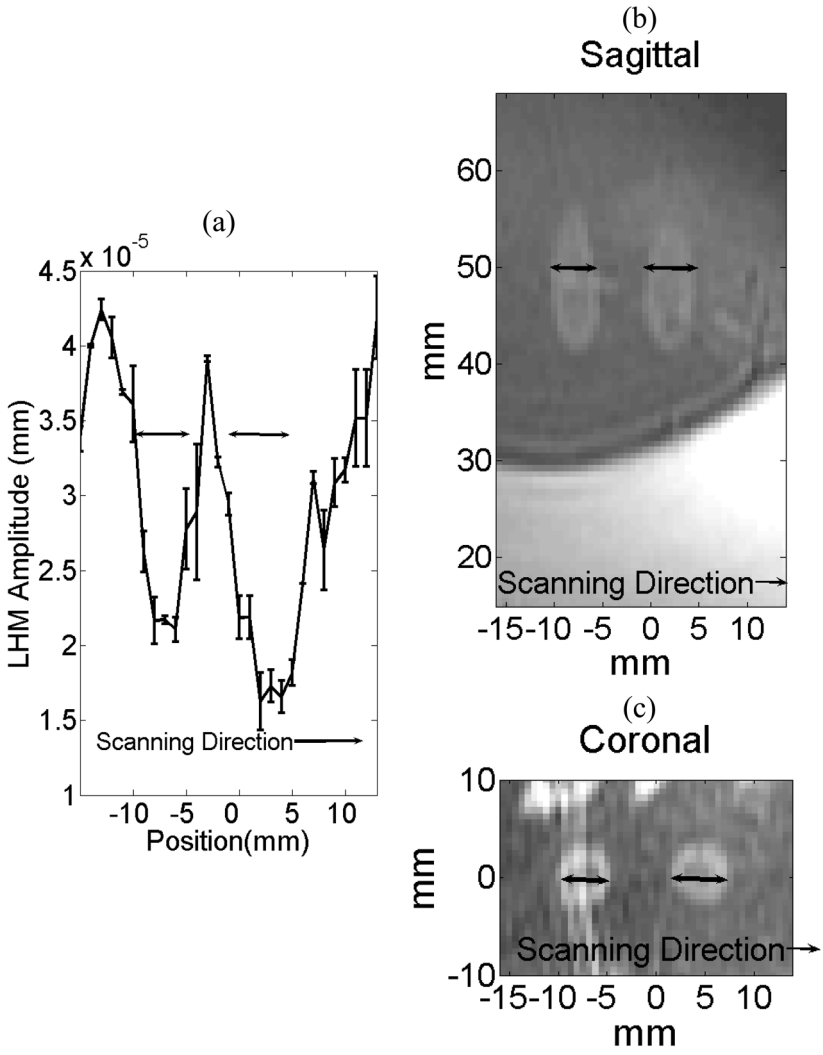

Figure 10.

Spatial LHM scan after two sonications (at locations Nos. 13 and 14) and the corresponding sagittal and coronal T2-weigthed MR images. The focus of the FUS transducer was located at the same vertical position for both sonications (at 50 mm in the sagittal image). The sonications were made 10-mm apart following the scan direction (superior/inferior). (a) Value of the LHM amplitude following the scanning direction. Corresponding T2-weighted sagittal (b) and coronal (c) MR images of the lesions.

Table 1

Sonication parameters used for the experiments. The sonication was made at an acoustic power of 22.5 W (time-averaged) during 40 s with pauses between bursts in order to vary the total exposure time (ON time). The burst frequency was 100 Hz with a 50% duty cycle.

	Acoustic Intensity at Focus (W/cm^2)	Focal depth (mm)	Total ON time (s)	Rabbit/Leg
1	1300	23.6	20	1/Left
2	1400	22	20	1/Left
3	1300	22.9	20	1/Right
4	1300	22.7	20	2/Right
5	1400	21	12.8	2/Right
6	1300	25.4	16.4	3/Left
7	1500	13.3	17.2	3/Left
8	1500	14.9	14.8	3/Left
9	1400	20.3	15.6	3/Left
10	1400	18.3	20	3/Left
11	1500	17.3	17.4	3/Left
12	1300	23.2	20	3/Right
13	1400	20.7	14.4	3/Right
14	1400	19.1	16.4	3/Right

Table 2

Controlled exposure experiments results. The LHM measurements were made every 1.1 s with a burst modulation frequency of 75 Hz and a 50% duty cycle. The threshold value for the controlled exposure was calculated as LHM average amplitude − 2* standard deviation (SD).

	Acoustic Intensity at Focus for LHM measurements (W/cm^2)	for lesion formation (W/cm^2)	Focal depth (mm)	LHM Average Amplitude ± SD (μm)	Time to reach threshold (s)	Observation
1	2600	2900	17.2	33±6	16.2	Coagulation
2	2000	2100	17.7	43±5	7.3	Coagulation
3	2200	2300	10.4	36±4	14.2	Coagulation
4	2000	2000	21.4	22±2	21.9	Coagulation
5	2000	2000	19.6	26±2	10.6	Coagulation
6	2000	2000	19.7	25±3	8.2	Coagulation
7	2000	2100	17.5	28±1	12.0	Coagulation
8	2000	1900	22.6	26±2	9.9	Coagulation
9	1900	1900	26.3	24±2	10.1	Coagulation
10	2400	1900	22.6	20±1	22.3	Coagulation
11	2100	1900	25	23±3	15.6	Coagulation
12	2400	1900	23.7	19±1	9.8	Coagulation
13	2300	2000	18.8	21±2	6.0	Coagulation
14	2300	2100	16.9	24±2	16.2	Coagulation
15	2400	2200	13.2	26±2	10.0	Coagulation
16	2700	2100	14.6	25±2	6.1	Coagulation
17	2500	2100	16.4	24±1	—	Stopped Immediately
18	2400	2000	19.4	25±3	32.1	Coagulation
19	2200	2000	19.4	31±6	6.0	Coagulation
20	2900	2000	19.7	23±2	13.6	Coagulation
21	2200	2000	19.8	32±2	—	Stopped Immediately
22	2600	2100	16.8	21±3	11.9	Coagulation
23	2000	2100	17.4	39±4	—	Stopped Immediately
24 [a]	2000	2100	17.9	23±1	—	Stopped Immediately (+5s)
25 [a]	3300	2100	18.1	22±2	27.1	Coagulation (+5s)
26 [a]	3100	2100	15.6	29±2	13.8	Coagulation (+5s)
27 [a]	3100	2100	15.6	23±1	—	Did not stop (50s)
28 [a]	3400	2200	12.6	19±4	—	Did not stop (50s)
29 [a]	2300	2000	19.1	20±4	27.6	Coagulation (+5s)
30 [a]	2600	2100	16.2	36±4	4.0	Coagulation (+5s)
31 [a]	2600	2100	17	29±6	11.7	Coagulation (+5s)
32	2700	2000	21.5	32±3	—	Stopped Immediately
33	2700	1900	23.5	27±2	13.1	Coagulation
34	2800	2000	19.6	26±1	10.3	Coagulation
35	2700	1900	22.3	28±1	4.0	Coagulation
36	1600	1600	20.9	24±1	17.7	Coagulation
37	1700	1600	19.4	24±1	9.9	Coagulation
38	1700	1600	18	36±2	10.2	Coagulation
39	1900	1400	9.2	35±2	15.6	Coagulation
40	3200	1200	19.1	33±2	—	Stopped Immediately
41	3000	1200	17.3	31±2	24.8	Coagulation
42	3100	1300	15.3	34±4	16.1	Coagulation

[a] For these experiments the exposure was finished 5 s after reaching the threshold value.